Proceedings 10th NUMGE 2023
10th European Conference on Numerical Methods in Geotechnical Engineering
Zdravkovic L, Kontoe S, Taborda DMG, Tsiampousi A (eds)

https://doi.org/10.53243/NUMGE2023-173

Derivation of equivalent number of cycles in the design of cyclically loaded offshore foundations

J.-E. Saathoff[1], M. Achmus[1]

[1]*Institute for Geotechnical Engineering, Leibniz University Hannover, Germany*

ABSTRACT: Especially during storm events, excess pore pressure can build up in the soil around cyclically loaded offshore foundations. Such accumulated excess pore pressure reduces the effective stresses in the soil and thus has a negative impact on structural integrity. In this work, a practical approach is presented to apply the soil behaviour determined in cyclic direct simple shear tests to the bearing capacity of the foundation structure using a three-dimensional numerical model. In practical designs, not a single load package with a constant number of equivalent cycles is given, but a design storm with different storm bins. The presented numerical approach is complemented by a procedure to derive an equivalent number of cycles from predefined load parcels. The soil response is accounted for by a contour approach that allows the use of site-specific cyclic direct simple shear test results by considering the mean stress, the cyclic shear stress amplitude and the number of load cycles at each integration point of the numerical model under partially drained conditions.

Keywords: contour; cyclic loading; excess pore pressure; equivalent number of cycles; offshore

1 INTRODUCTION

During storm events, excess pore pressure may be accumulated due to a relatively fast loading and a limited surrounding permeability. The subsequent reduction in effective stresses influences the capacity and deformation of large monopile foundations in sandy material. For the estimation, mainly finite element models with a predefined number of equivalent cycles are used in academia and practice. Besides implicit models, which calculate each cycle individually with sophisticated constitutive models (Liu et al. 2021), often explicit calculations are performed. Models that base on this method are for example the High Cycle Accumulation model (HCA) (Niemunis et al. 2005) or the UnDrained Cyclic Accumulation Model (UDCAM) with the extension to the Partially Drained Cyclic Accumulation Model (PDCAM) (Jostad 1997, Andersen 2015). In contrast to these models, a method termed EPPE which puts special focus on practicability was developed by Achmus et al. (2018).

Since a cyclic loading event consists of irregular cyclic loads of different magnitudes and load types, additionally, a concept to consider the complete irregular storm load is needed. This concept is implemented into the EPPE approach to enhance its applicability. The procedure is described in Achmus et al. (2018) and Saathoff et Achmus (2021). The irregular storm can be transformed into a regular storm load using rainflow counting (Matsuishi et Endo 1968). The storm load and the corresponding equivalent number of cycles must have the same final effect on the soil-structure interaction as the irregular storm load. However, the trend over time may not be the same. In the numerical procedure, special focus was put on the practicability as well as the determinability of interim steps with engineering judgement.

Regarding the cyclic soil response on element level for sandy soils, some definitions are necessary. The absolute excess pore pressure Δu is normalized for the cyclic direct simple shear case by the vertical consolidation stress σ'_{vc} to the excess pore pressure ratio R_u:

$$R_{u,DSS} = \Delta u/\sigma'_{vc} \quad (1)$$

The build-up trend of the excess pore pressure depends on the applied shear stress τ, which can be characterised with the cyclic stress ratio (CSR) and the mean stress ratio (MSR) (Equations 2 and 3). Therefore, the acting shear stress load is divided into mean component τ_{mean} and a shear stress amplitude τ_{cyc} (similar to the mean load and the load cyclic amplitude in Figure 5).

$$CSR_{DSS} = \tau_{cyc}/\sigma'_{vc} \quad (2)$$
$$MSR_{DSS} = \tau_{mean}/\sigma'_{vc} \quad (3)$$

2 REFERENCE MODEL

The numerical method shall be explained on a reference monopile with a diameter of 9 m and an embedded length of 27 m with a wall thickness of 10 cm. The load eccentricity is 40 m. The acting fictitious storm load is depicted in Figure 1. Herein, the load amplitude and the mean load component are depicted over the number of cycles for the respective storm bin. Large loads occur with a small number of cycles and small loads with a large number of cycles. But all loads have the same eccentricity. The soil is layered with alternating sand and clay layers. The layering and the soil properties are shown in Tables 1 and 2.

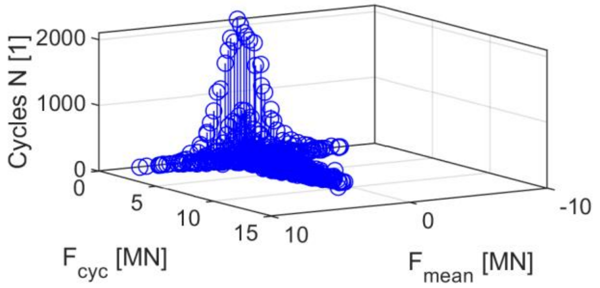

Figure 1. Fictitious storm load

Table 1. Soil layering

Soil	Depth	Cyclic response
Sand	0 m - 5 m	Figure 2
Clay	5 m - 10 m	Figure 3
Sand	10 m - 15 m	Figure 2
Clay	15 m - 20 m	Figure 3
Sand	20 m - 50 m	Figure 2

Detailed information on the numerical finite element model can be found in Achmus et al. (2018). The investigation is carried out in ABAQUS (Dassault Systèmes 2016) with a relatively simple elastoplastic constitutive law with Mohr Coloumb failure criterion. The dimensions of the model and mesh resolution were investigated in preliminary investigations. The stiffness is considered stress-dependent with a reference stiffness $E_{s,ref}$ and a stiffness exponent governing the stress-dependence.

Table 2. Soil properties

Property	Unit	Sand	Clay
Cohesion c‘ /c_u	[kN/m²]	0.1	100
Buoyant unit weight γ'	[kN/m³]	10	9
Friction angle φ‘	[°]	40	0.0
Dilatancy ψ	[°]	10	0.0
Poisson’s ratio ν	[1]	0.25	0.45
Stiffness $E_{s,ref}$	[MN/m²]	70	30
Stiffness exponent	[1]	0.5	0.8
Permeability k_f	[m/s]	3e-4	1e-6

The cyclic soil response is considered based on contour plots. This can be derived from cyclic direct simple shear or cyclic triaxial tests. The Mohr-Columb soil model is only used in order to estimate the stresses in each integration point and derive the prevailing CSR value. In the contour plot, the CSR is plotted over the number of cycles for different excess pore pressure ratio isocurves. In Figure 2, the maximum value is $R_u = 0.95$, which is achieved in the element test with an increasing number of cycles for smaller shear loads. The CSR (and MSR) is normalized in cyclic direct simple shear tests for sand with the vertical consolidation stress and for cohesive material with the undrained shear strength. Finally, the excess pore pressure ratio depending on MSR, CSR and the number of equivalent cycles can be read from these plots in order to consider the cyclis soil response.

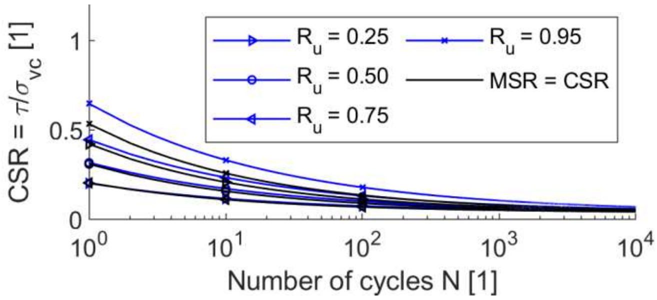

Figure 2. Contour plot for a sand layer with MSR = 0 and CSR = MSR for the same isocurves in dotted black

Figures 2 and 3 show exemplary contour plots for symmetric two-way loading (MSR = 0) and one-way loading with full unloading (MSR = CSR) for sand and clay, respectively. Herein, only four isolines for the excess pore pressure ratio are plotted. For an increasing MSR, the number of cycles, for which large excess pore pressure ratios are derived, decreases for the same CSR value.

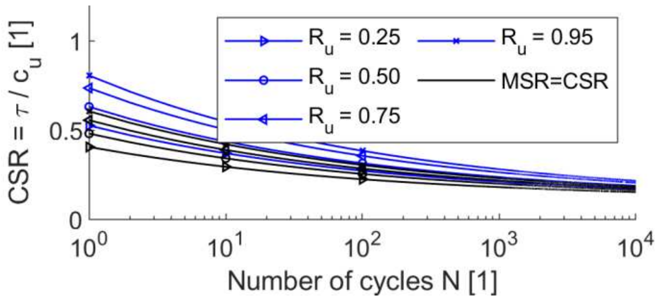

Figure 3. Contour plot for clay layer with MSR = 0 and CSR = MSR for the same isocurves in dotted black

3 EPPE CONCEPT

The excess pore pressure estimation concept was explained in Achmus et al. (2018) and was further developed. Different storm bins can be calculated one after the other to consider the complete storm load. Instead of this complex calculation procedure, however, compatibility can also be ensured by using the excess pore pressure ratio as a memory variable in combination with contour plots (cf. Andersen 2015). The excess pore pressure at the end of a cycle is equal to the excess pore pressure at the beginning of the next cycle. It can hence be used to calculate the number of equivalent cycles through the storm. However, for sandy material drainage needs to be considered. For an offshore foundation this should be done on element system level considering spatial dissipation effects.

The approach presented consists of several calculation steps. The maximum reference load is applied in a finite element model to read the stress components for each integration point. In the following, the estimation procedure shall be explained in greater detail.

3.1 General

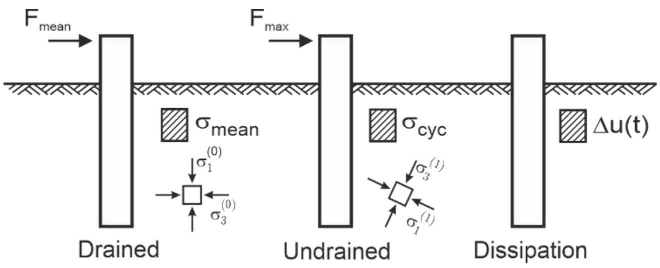

Figure 4. EPPE concept

In the concept, the monopile is loaded with a mean load and subsequently with the load amplitude (Figure 4). The load amplitude is also applied under drained conditions. The step, in which the storm amplitude is considered, is termed undrained in Figure 4, because a fast load application is assumed. The principal stresses in each integration point are read and from these equivalent stress values are derived. Therefore, Equations 4 and 5 are used. The octahedral stress is used for normalization purposes and the equivalent shear stress to derive a representative value for the acting shearing in the integration points.

$$\sigma'_{oct} = (\sigma'_1+\sigma'_2+\sigma'_3)/3 \quad (4)$$

$$\sigma'_{eq} = ([(\sigma'_1-\sigma'_2)^2+(\sigma'_2-\sigma'_3)^2+(\sigma'_3-\sigma'_1)^2]/2)^{0.5} \quad (5)$$

3.2 Sorting

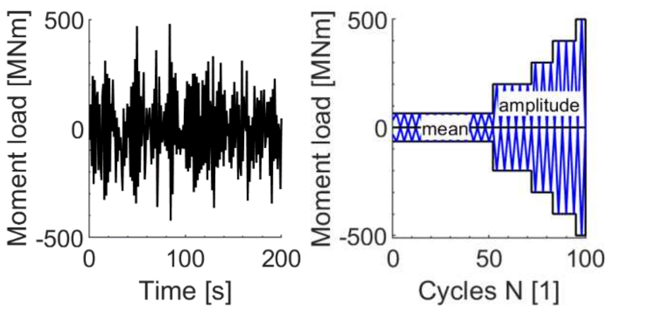

Figure 5. Schematic of transfer of storm load from irregular (a) to regular (b) storm bins

The irregular storm load is transferred to storm bins with constant mean load and load amplitude with a related number of cycles (Figure 5). Each storm bin in the example of Figure 5 (b) has a number of cycles and maximum and minimum storm load.

The storm load needs to be sorted in a way that the most severe load is the last storm entry. Therefore, the stresses which have been stored for each load condition in each integration point are processed as depicted in Figure 6. The octahedral stress and equivalent shear stress are interpolated for each storm load bin with the related global mean and maximum load. The octahedral stress starts with a value related to the initial consolidation stress of 37 kPa for a depth of -4.5 m. The deviator in terms of the equivalent shear stress is calculated to be 13 kPa for initial conditions. The stresses are interpolated, among others, for the maximum storm load of 14 MN with a mean load of 1 MN. This load is hence an almost symmetric two-way loading.

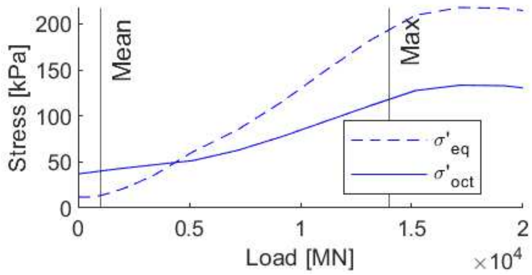

Figure 6. Stresses over calculation (global load) at symmetry axis for a point 2 m in front of the monopile (in loading direction) and at a depth of -4.5 m below mudline

From the interpolated stresses, the CSR and MSR can be calculated for finite element conditions according to Equations 6 to 9. These are derived from the stresses in each integration point. The CSR and MSR values are different in each storm bin.

$$CSR_{FE,sand} = (\sigma'_{eq,Fmax} - \sigma'_{eq,Fmean})/(2\ \sigma'_{oct,Fmean}) \quad (6)$$

$$MSR_{FE,sand} = (\sigma'_{eq,Fmean} - \sigma'_{eq,Fmin})/(2\ \sigma'_{oct,Fmean}) \quad (7)$$

$$CSR_{FE,clay} = (\sigma'_{eq,Fmax} - \sigma'_{eq,Fmean})/(2\ s_u) \quad (8)$$

$$MSR_{FE,clay} = (\sigma'_{eq,\ Fmean} - \sigma'_{eq,\ Fmin})/(2\ s_u) \quad (9)$$

The CSR and MSR for non-cohesive soils under finite element conditions are transferred to direct simple shear conditions by using the earth pressure coefficient at rest (Equation 10).

$$\sigma'_{oct} = \sigma'_v\ (1+2\ k_0)/3 \quad (10)$$

The spatial distribution of the CSR field for the largest storm load under symmetric two-way loading is shown in Figure 7. The largest CSR values are in front of the pile. Also, the soil layering can be seen, because there is a different response in terms of bedding reaction and hence different stress distributions. Soil elements with CSR values larger than the one from the related contour plots are assumed to be liquefied after one cycle.

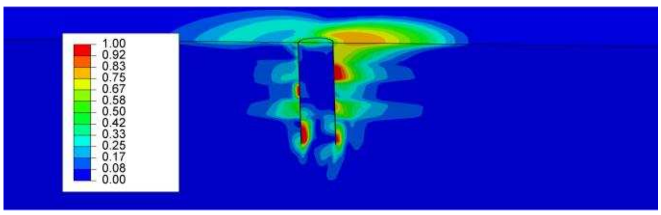

Figure 7. CSR field for largest storm load

With the CSR and MSR fields for each storm load bin, the excess pore pressure can be derived by using the contour plots from Figures 2 and 3. The related number of cycles is given for each storm bin (cf. Figure 1). The excess pore pressure ratio calculated from direct simple shear test results is interpreted under finite element conditions as shown in Equations 11 and 12.

$$R_{u,sand} = \Delta u / \sigma'_{oct,Fmean} \quad (11)$$

$$R_{u,clay} = \Delta u / c_u \quad (12)$$

The excess pore pressure ratio R_u is interpreted as a damage indicator. The storm is reordered based on a calculated damage. Because the storm can be sorted in different ways, Figure 8 (a) shows the excess pore pressure ratio for the initial storm order. The maximum load or the maximum load amplitude does not necessarily induce the largest damage due to the interaction between the mean and the cyclic load components. The reordered storm in terms of the induced damage can be seen in Figure 8 (a). The CSR value in the sorted storm increases steadily and so does the excess pore pressure ratio (Figure 8). The maximum CSR value of 0.76 can also be seen in Figure 7 in light yellow.

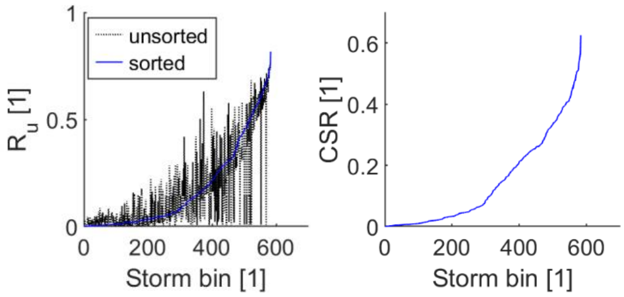

(a) *(b)*

Figure 8. Sorted storm load with R_u (b) and CSR (b) at symmetry axis for a point 3 m in front of the monopile (in loading direction) and at a depth of -4.5 m below mudline

Figure 9 shows the sorted global storm load and the number of cycles. The number of cycles decreases and the storm load increases, thereby, the last storm entry has 0.5 cycles under asymmetric two-way loading.

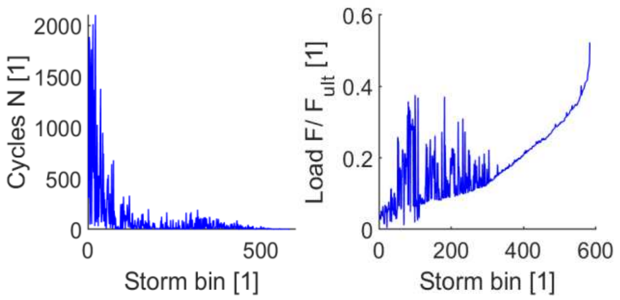

(a) *(b)*

Figure 9. Sorted global storm load with number of cycles in each bin (a) and the increase of load in comparison to the maximum storm load (b)

The sorting is done by assuming the validity of the Miner rule (Miner 1945, Palmgren 1924).

3.3 *Excess pore pressure for one cycle*

The general concept to use the excess pore pressure ratio as a history variable is explained in Figure 10. The excess pore pressure ratio is used to track the build-up over the storm loading. However, to reduce the computational effort, integration points were excluded which have CSR values smaller compared to a derived limit value. The limit value is derived for a number of cycles of 1000 for $R_u = 0.25$ and is interpreted as the asymptotic value in the contour plots (Figures 2 and 3). The influence was investigated in preliminary investigations. It has no physical justification and is only used to reduce the computational time. The idea is to consider also dissipation in the reference case and then consider subsequently the different storm bins. Therefore, first, the dissipation response is needed.

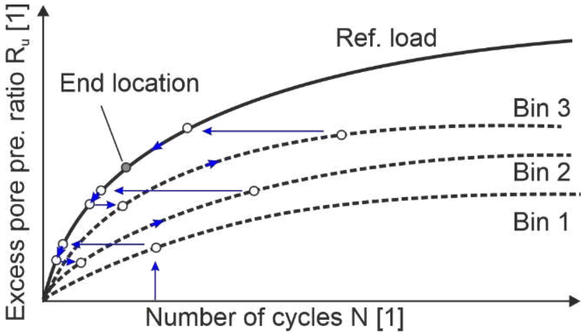

Figure 10. Concept to derive an equivalent number of cycles

To estimate the dissipation effect, the excess pore pressure ratio R_u (and the excess pore pressure) is derived for each integration point for one cycle and based on the stresses of the last entry of the newly sorted storm (F_{max} = 14 MN).

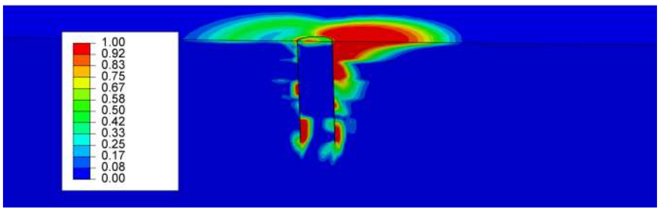

Figure 11. Excess pore pressure ratio R_u after one cycle

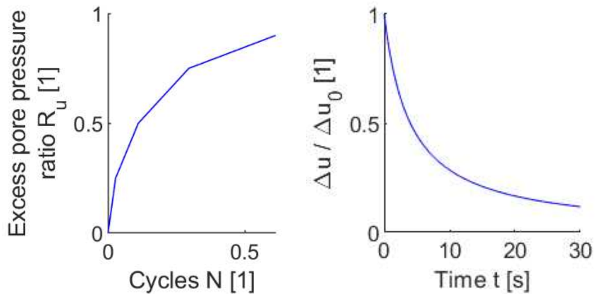

(a) *(b)*

Figure 12. Undrained excess pore pressure accumulation (a) and normalized decay curve (b) at symmetry axis for a point 3 m in front of the monopile (in loading direction) and at a depth of -4.5 m below mudline

The excess pore pressure ratio field after one cycle is depicted in Figure 11. The maximum damage can clearly be seen on the right (passive) pile side. A value of one represents theoretical liquefaction under completely undrained conditions. Figure 12 (a) shows the undrained response in terms of excess pore pressure ratio over the number of cycles for an exemplary point of the model.

3.4 Dissipation

The related excess pore pressure Δu field, denormalized from R_u with the $\sigma'_{oct,Fmean}$, is input in a coupled ABAQUS model and the field is dissipated over several seconds (more than the storm period T, which is assumed to be 10 s). The result is a decay curve for each integration point, which is normalized to be used in the analytical superposition (Figure 12 (b)).

The main information from Figure 12 (b) is the decrease of excess pore pressure after the storm period T in percent for that one location. The storm period is assumed constant to be 10 s, but can also be varied over the duration of the storm.

3.5 Superposition

To consider the number of cycles for one particular storm bin under partially drained conditions, a superposition is used. Herein, the decay curves obtained for the excess pore pressure field Δu after one cycle are applied. This is a model assumption for simplification reasons. However, no cyclic sequential calculations are necessary in this way. The conservative superposition method to consider the superposition is shown in Figure 13 with an examplary dissipation of 50%.

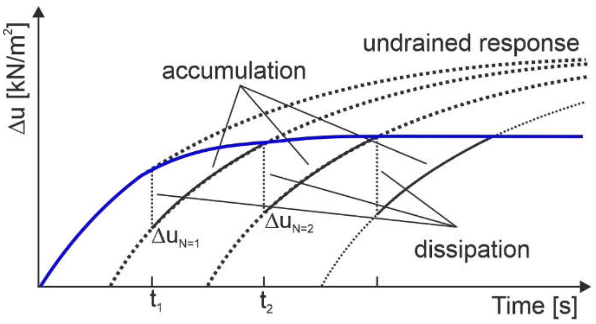

Figure 13. Analytical superposition method

The cyclic superposition of one storm bin uses mainly the large increase in the first part of the curve and is based on the idea that the remaining excess pore pressure after dissipation is calculated back to a new number of equivalent cycles in the curve itself. A new cycle is added to the equivalent number of cycles. For each cycle added, the excess pore pressure curve is only shifted in the x-direction. Changes in the build-up trend are not taken into account. The excess pore pressure ratio of the individual storm bin is transferred to the reference curve and a respective number of equivalent cycles. The number of cycles determines the number of superposition steps. Within the superposition, the starting value from the previous dissipation is used and an additional cycle is applied. The excess pore pressure increases. Afterwards, the resulting excess pore pressure is reduced by the value based on the dissipation analysis. If the number of cycles is smaller than one only this fraction is applied. The procedure is repeated for the number of equivalent cycles. The excess pore pressure increases due to an additional number of undrained cycles and decreases due to dissipation. After some cycles, a stable equilibrium is reached and no increase occurs. However, in this way, only one storm bin and not the complete storm with many regular storm packages is considered.

3.6 Consideration of the complete storm

Figure 10 shows the required procedure which is combined with the superposition in Figure 13. First, the excess pore pressure ratio for the number of cycles of the first storm bin, for each point depending on CSR and MSR, is derived (Figure 10 first circle for bin 1).

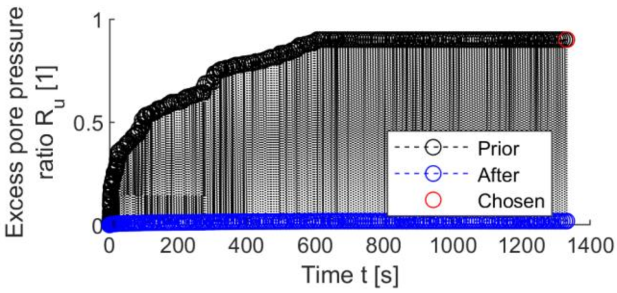

Figure 14. Excess pore pressure ratio build-up at symmetry axis for a point 3 m in front of the monopile (in loading direction) and at a depth of -4.5 m below mudline

An equivalent number of cycles after dissipation can be derived from the residual excess pore pressure ratio with a specific R_u-N curve of the undrained reference curve (Figure 10 path from bin 1 to reference load; Figure 12 (a)). The superposition method is performed and the residual excess pore pressure ratio is transferred to the next storm bin (Figure 10 from reference load to bin 2). The number of equivalent cycles within this curve is derived and the number of cycles from the next storm bin is added to the number of cycles of the last storm entry (cf. Figure 10). Afterwards, the excess pore pressure ratio of the storm entry is again transferred to the reference curve (not the largest load, but the storm entry with the largest induced damage) and an analytical superposition is performed. The procedure is done for all subsequent storm entries. The excess pore pressure ratio after dissipation as well as the related number of equivalent cycles after dissipation are now known.

The excess pore pressure ratio over the storm bins is shown in Figure 14 for a point 1/3D in front of the pile and 0.5D below mudline. First, no excess pore pressure accumulates due to very small global loads. For larger loads at the end of the storm, the excess pore pressure accumulates because it cannot dissipate fast enough and subsequently reduces the bedding reaction. As a conservative assumption, in the following the dissipation of the last step is neglected (red dot in Figure 14).

3.7 *Post-cyclic capacity*

The final excess pore pressure ratio field is shown in Figure 15. The induced damage in terms of excess pore pressure is smaller compared to the field under undrained conditions after one cycle. Most of the damage is dissipated due to the large hydraulic conductivity in the sand layers. The layering can also clearly be seen, which results from different dissipation and excess pore pressure generation responses in the different soil types.

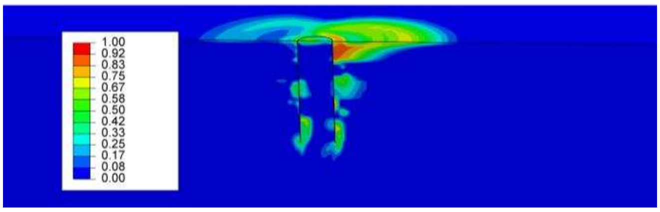

Figure 15. Final excess pore pressure ratio R_u

The angle of internal friction and undrained shear strength are reduced by the induced damage in order to consider the decrease in effective consolidation stress due to excess pore pressure accumulation (see Achmus et al. 2018) (Equations 13 and 14).

$$\varphi'_{red} = \arctan(\ (1-R_u)\ \tan(\varphi')\ ) \qquad (13)$$

$$c_{u,red} = (1-R_u)\ c_u \qquad (14)$$

The resulting load-displacement curve at mudline is shown in Figure 16. There is a softer soil response with a capacity degradation of 30% for this fictitious example.

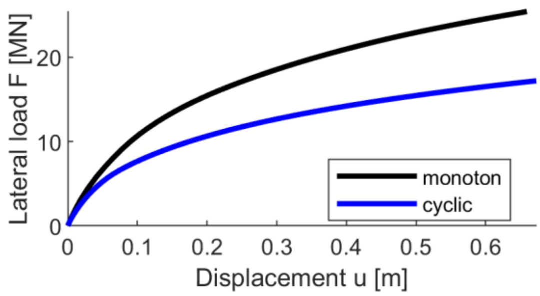

Figure 16. Load-displacement curve for reference monopile system with monotonic and cyclic response at mudline

4 CONCLUSIONS

Due to non-linear effects and spatial influences in the soil-structure interaction, it is almost impossible to estimate the cyclic soil response with analytical methods with a reasonable accuracy for an optimized design. Therefore, finite element models are needed. A procedure was described with an example of a layered soil to consider capacity degradation with the consideration of a complete storm. The method can quantify the cyclic capacity degradation due to storm loads by also considering the complete storm build-up. It can stepwise be assessed and it is simple to use. Although there are several model assumptions for simplification reasons, the estimation can be seen as conservative (Saathoff 2022) and is therefore quite useful. By using contour plots the cyclic element degradation can be assessed very fast. The EPPE procedure focuses on transparency and practical applicability. It is in accordance with DNV (DNV-RP-C212). The procedure can calculate the post-cyclic response relatively fast and is hence able to realize calculations for a complete wind farm in a reasonable time span. The stiffness degradation can also be considered, but this was not explained in this work. Due to its modular framework, individual steps can be exchanged for more sophisticated analyses.

5 ACKNOWLEDGEMENTS

The investigations reported were funded by the Deutsche Forschungsgemeinschaft (DFG, German Research Foundation) - SFB1463 – 434502799. The support is gratefully acknowledged.

6 REFERENCES

Achmus, M., Saathoff, J.-E. and Thieken, K. 2018. *Numerical method for evaluation of excess ore pressure build-up at cyclically loaded offshore foundations*. In Numerical Methods in Geotechnical Engineering IX, 1461–1468. URL https://doi.org/10.1201/9781351003629-184.

Andersen, K. H. 2015. *Cyclic soil parameters for offshore foundation design*. The 3rd McClelland Lecture. In Meyer, editor, Frontiers in Offshore Geotechnics III, ISFOG 2015, volume 1, 5–82. Taylor & Francis Group, London.

Dassault Systèmes. Abaqus 2016. 2016.

DNV-RP-C212. 2019. Offshore soil mechanics and geotechnical engineering. Standard, Det Norske Veritas.

Jostad, H. P., Andersen, K. H. and Tjelta, T. I. 1997. *Analyses of skirted foundations and anchors in sand subjected to cyclic loading*.

Liu, H., Kementzetzidis, E., Abell, J. A. and Pisanò, F. 2021. *From cyclic sand ratcheting to tilt accumulation of offshore monopiles: 3D FE modelling using SANISAND-MS*. Géotechnique, 72(9):753–768. URL https://doi.org/10.1680/jgeot.20.P.029.

Matsuishi, M. and Endo, T. 1968. *Fatigue of metals subjected to varying stress*. Presented to the Japan Society of Mechanical Engineers.

Miner, M. A. 1945. *Cumulative damage in fatigue*. Journal of Applied Mechanics, 12(3):159–164. URL https://doi.org/10.1115/1.4009458.

Niemunis, A., Wichtmann, T. and Triantafyllidis, T. 2005. *A high-cycle accumulation model for sand*. Computers and Geotechnics, 32(4):245–263. URL https://doi.org/10.1016/j.compgeo.2005.03.002.

Palmgren, A. G. 1924. *Die Lebensdauer von Kugellagern*. Zeitschrift des Vereines Deutscher Ingenieure (ZVDI), 14:339–341. (in German).

Saathoff, J.-E. and Achmus, M. 2020. *Practical approach for the evaluation of cyclically induced excess pore pressure around offshore foundations in sand*. In Proceedings of the 4th International Symposium on Frontiers in Offshore Geotechnics.

Saathoff, J.-E. 2022. *Modelling of excess pore pressure accumulation in sand around cyclically loaded foundations*. PhD thesis. Leibniz University Hannover.